

Image-based ECG Sampling of IVUS Sequences

Aura Hernández, David Rotger and Debora Gil
 Computer Vision Center and Department of Computer Science
 Universitat Autònoma de Barcelona
 Bellaterra, Spain
 aura,debora@cvc.uab.es

Abstract—Longitudinal motion artifacts in IntraVascular UltraSound (IVUS) sequences hinders a properly 3D reconstruction and vessel measurements. Most of current techniques base on the ECG signal to obtain a gated pullback without the longitudinal artifact by using a specific hardware or the ECG signal itself. The potential of IVUS images processing for phase retrieval still remains little explored. In this paper, we present a fast forward image-based algorithm to approach ECG sampling. Inspired on the fact that maximum and minimum lumen areas are related to end-systole and end-diastole, our cardiac phase retrieval is based on the analysis of tissue density of mass along the sequence. The comparison between automatic and manual phase retrieval (0.07 ± 0.07 mm. of error) encourages a deep validation contrasting with ECG signals.

Keywords: Longitudinal Motion, Image-based ECG-gating, Fourier analysis

I. INTRODUCTION

IntraVascular Ultrasound (IVUS) is a catheter-based technique which shows cross sections of arteries and enables 3D visualization and measurements of coronary arteries. A major drawback during in vivo acquisitions is that the catheter moves in and out the artery due to heart beat. This swinging effect hinders 3D reconstruction and measurements [1]. Figure 1 shows an example of longitudinal motion artifact. A shadow appearing and disappearing on the left hand side of the image hinders the continuous visualization of the lumen and vessel wall. At the final of the sequence, on the right hand side of the image, the movement of the catheter in and out provokes that plaque appears and disappears (on the top half of the cut).

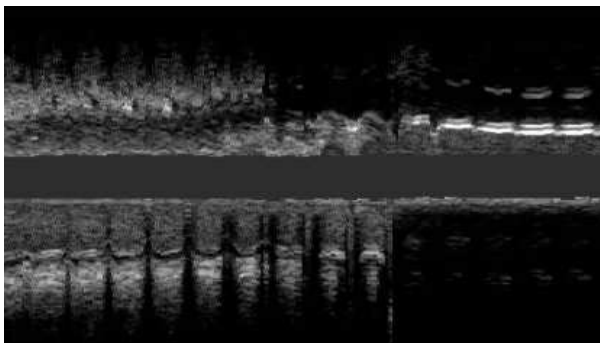


Figure 1. Swinging effect reflected in a longitudinal cut.

Longitudinal motion artifacts might be overcome by ECG-gating sequences, which return a static sequence synchronized

with cardiac phase [2]. Synchronization can be performed either on-line during acquisitions [3] or off-line by processing a standard non-gated sequence [4]. On-line procedures require a specific hardware (not always available) for acquiring frames at end-diastole. Off-line techniques require delicate process of the ECG signal for extracting a sequence sampling synchronized at end-diastole given by ECG-peaks. In any case, a simultaneous acquisition (not supported by all commercial devices) of IVUS images and ECG-signal is required.

Although IVUS images dynamics (such as lumen area extrema or rotation angle) reflect cardiac motion, the potential of IVUS images processing for phase retrieval still remains little explored. Existing strategies [5]–[7] follow the scheme sketched in figure 2. First, a signal reflecting cardiac motion



Figure 2. Pipeline for Image-based Cardiac Phase Retrieval.

is computed from IVUS sequences. Second, the signal is filtered (in the Fourier domain) in order to remove non-cardiac phenomena and artifacts. Finally, suitable sampling of the filtered signal retrieve cardiac phase. Based on clinical studies [8] and physical properties [9], all authors agree in using the extrema of filtered signals for sampling at end-systole and diastole. The main differences among existing algorithms (and, thus, the clue for an accurate cardiac phase retrieval) are on the signal computed from the sequence and the filter used to extract the cardiac profile. Nadkarni et al. [5] bases their approach on the changes of lumen size. Zhu et al. [6] propose two different methods, based on average intensity and absolute intensity difference of images along the sequence, to extract the signal containing cardiac phase. Meanwhile, Matsumoto et al. [7] also study different standard similarity measures along the sequence to compute a signal, which is further filtered using wavelets for cardiac profile retrieval.

This paper presents a fast approach to image-based ECG sampling. The method explores the conservation of density of mass of the vessel along the sequence to detect abrupt changes, which are consequence of cardiac motion and morphological changes. In order to reduce noise due to morphological changes, the method adopts a local approach by computing the density of mass over a neighborhood of a set of pixels reflecting motion. Two different band-pass filters are used to retrieve cardiac profiles: Butterworth and Gabor. The results

suggest that the Gabor-based sampling is better.

The paper is organized as follows. The cardiac phase retrieval is given in section II, validation in section III and discussion and conclusions in section IV.

II. METHOD

According to research in Shaw et al. [8], minimum and maximum lumen areas correspond to the beginning of the QRS complex (end-diastole) and T-wave peak (end-systole) of the ECG signal. By the physical coupling [9], lumen area evolution is related to other phenomena induced by cardiac motion.

Due to the ultrasound properties, image intensity reflects the density of mass and, thus, changes along the sequence either come from morphological changes or contain information about cardiac phase. In order to minimize the impact of image areas not reflecting cardiac motion (noisy and echo-shadowed), we adopt a local approach as in [10]. The image local mean (LM) along the sequence provides each pixel with a signal (step 1 in scheme of figure 2), prompt to contain information on cardiac phase. The signals LM serve to retrieve it in 3 steps:

- 1) **Selection of points reflecting motion:** Vessel motion is not reflected in the whole vessel section, but only at some salient areas such as plaque or vessel walls. Thus, we only analyze LM from those pixels reflecting motion by an optical filtering on \widehat{LM} which selects them.
- 2) **Extraction of Cardiac motion profile:** Since cardiac phase is not constant along the sequence, the LM profile computed from the above point is filtered. A band-pass filter on \widehat{LM} controls the regularity of the signal.
- 3) **Retrieval of Cardiac Phase:** In order to retrieve a unique cardiac phase from the image, a combination of cardiac phases from relevant pixels is computed.

The extraction of cardiac frequency, namely ω_c , is necessary for the first two steps. We define ω_c as the most prominent local maximum in the interval $I_{\omega_c} = (45, 200)$ repetitions per minute of the Fourier development of LM [11]. For the sake of an efficient algorithm, ω_c is approximated by the global maximum of \widehat{LM} amplitude for frequencies in the range I_{ω_c} . This process provides a ω_c for each image pixel. The average of all ω_c for a uniform sample of pixels constitutes our approximation to cardiac frequency.

The main steps of the algorithm are:

- 1) **Selection of points reflecting motion.** Since cardiac motion is a periodic signal, \widehat{LM} for those pixels reflecting motion should be as close to a discrete series (given by ω_c multiples) as possible. Other dynamic phenomena, such as breathing, morphological changes along the sequence and irregularities in heart beat distort the ideal discrete profile. In particular, the theoretic harmonic peaks result in a set of peaks spread around ω_c harmonics. The more irregular the profile is, the more spread around the theoretic harmonic the harmonics of \widehat{LM} are. We consider that points reflecting cardiac motion are those points which its \widehat{LM} has a well-defined

harmonic frequencies profile and, at the same time, \widehat{LM} has a large amplitude at ω_c .

From the initial uniform sampling of pixels, only those points with cardiac amplitude over the 80% percentile of all \widehat{LM} amplitudes are considered. This set will be noted by \mathcal{MP} .

There might be pixels with a large amplitude but an irregular profile, so that they do not reflect cardiac motion. We remove those pixels by means of an optical filtering [12] on the principal harmonic ω_c . Optical filtering selects only those Fourier relevant peaks by thresholding the difference between the amplitude achieved at the harmonic and an average of neighboring amplitudes. Figure 3 shows an example of two different profiles from two points. The first profile reflects cardiac motion, while the second one is an irregular profile which does not present any distinguished harmonic.

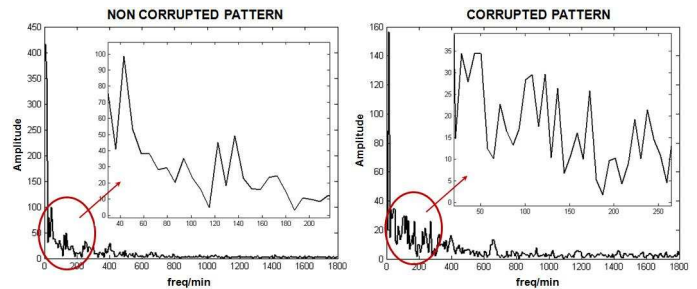


Figure 3. Regular profile (left) versus irregular profile (right). Optical filtering removes those profiles corrupted by noise from \mathcal{MP} set

The signals reflecting cardiac motion are given by the optical filtering of LM signals computed in the set \mathcal{MP} .

- 2) **Extraction of cardiac motion profile.** Even in healthy subjects, cardiac frequency does not keep constant along the sequence, which introduces (among other phenomena) irregularities in \widehat{LM} . In order to smoothly approximate the cardiac profile, \widehat{LM} should be filtered. We model the extraction of cardiac phase by filtering \widehat{LM} with a bandpass filter. In this paper, we present two different filters: Butterworth (B) [6] and Gabor (G) [7]. Both of them are centered at the cardiac frequency ω_c and only filter the principal harmonic. The filters are defined as follows:

$$B(\omega) = \frac{1}{\sqrt{1 + \left(\frac{|\omega| - \omega_c}{0.6\Delta\omega_c}\right)^{2n}}}$$

$$G(\omega) = \frac{1}{\sigma\sqrt{2\pi}} e^{-(|\omega| - \omega_c)^2 / (2\sigma^2)}$$

with $\Delta = 0.5$ and $n = 4$ for Butterworth filter and $\sigma = 0.5$ for Gabor filter.

- 3) **Retrieval of Cardiac Phase.** Maximums and minimums of each filtered signal give a sampling at end-systole and end-diastole and, thus, retrieve cardiac phase for each selected pixel. However, since these signals can suffer small variations due to different cardiac contributions and ω_c slightly varies from one pixel to another, a unique cardiac phase for sequence retrieval is needed. We extract a single signal by averaging all filtered signals for selected pixels.

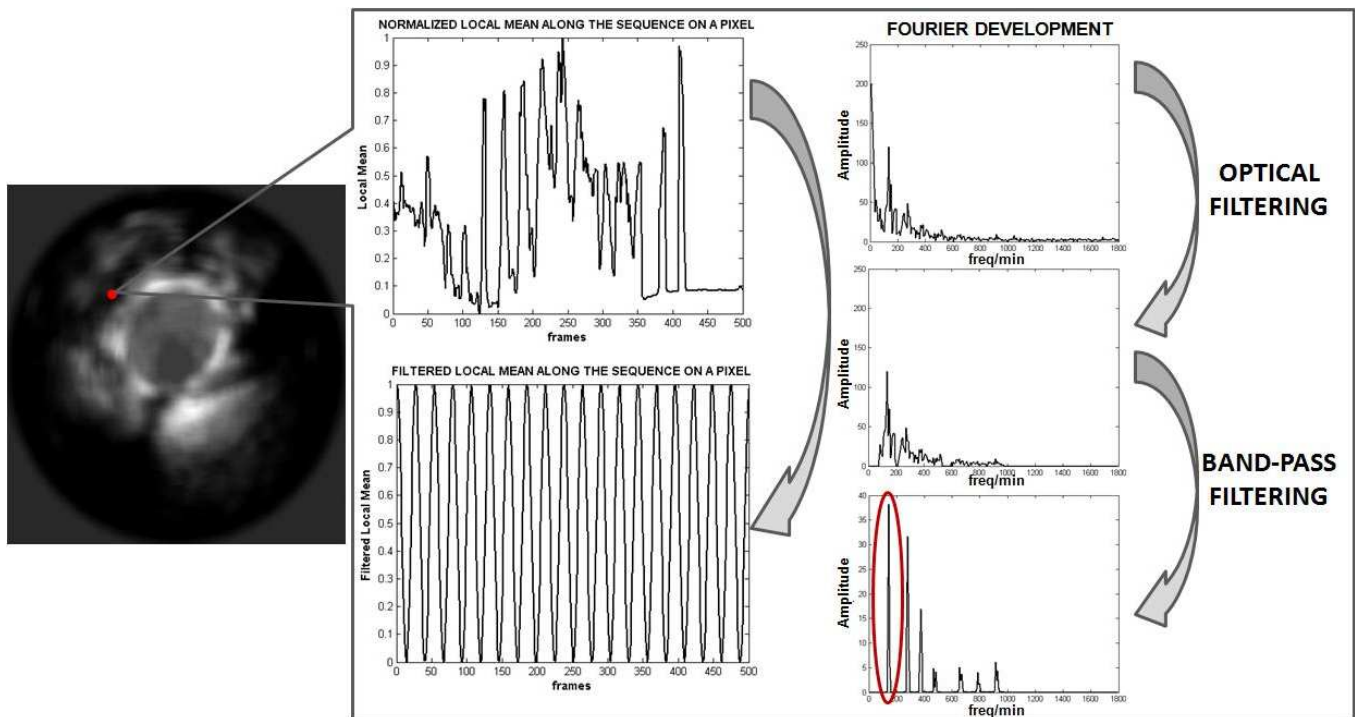


Figure 4. Main steps for extracting cardiac motion profile. On the left hand side of the figure, the Local Mean computation for an image. On the right hand side, the process to filter the local mean for a pixel along the sequence.

Figure 4 sketches the first two steps of the algorithm, once the first selection of pixels reflecting cardiac motion is done. On the left hand side of the figure, the local mean of an image is shown. From each pixel in \mathcal{MP} set (red point on the image), its local mean along the sequence is extracted (top plot on the middle of the figure). The Fourier development of this signal is shown on the top plot of the right hand of the figure. An optical filtering assures that the selected pixel reflects cardiac motion. In the case that this pixel had a signal corrupted by noise, it would be removed from the \mathcal{MP} set. For the pixels of \mathcal{MP} set with a non corrupted profile, a band-pass filter (Gabor in this figure) centered on the cardiac frequency ω_c applied to \widehat{LM} (bottom plot on the right hand side of the figure) regularize the signal. Finally, the real part of the inverse of the development, given only by the first harmonic is a smooth signal for the cardiac phase retrieval.

III. EXPERIMENTS

A. Experimental Setting

Our ECG-sampling method was been tested on eight segments between 400 and 500 frames long (6-8 mm approximately). Sequences were recorded using a Galaxy-BostonSci device at 40 MHz with a rotating single transducer and constant pullback (0.5 mm./sec.). The digitalization rate was 30 fps.

Automatic samplings were compared to the frames achieving extrema lumen areas. These extrema were manually detected by exploring longitudinal cuts. We selected minimums and maximums of intima/lumen and media-adventitia transition profiles. Figure 5 shows an example of manual samplings reflecting minimums of lumen area.

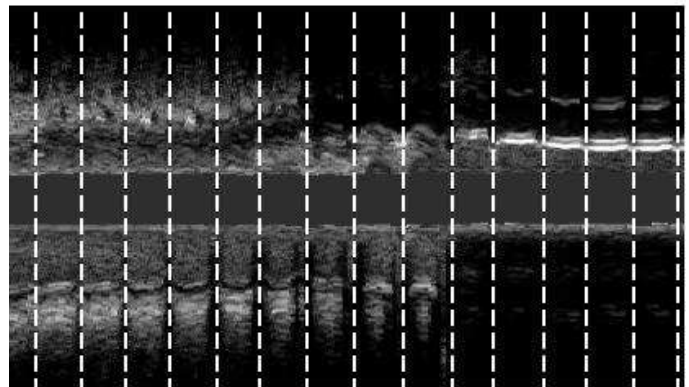


Figure 5. Manual Sampling for a Sequence

The distances between each manual detected frame and the automatic one most close to it were computed. That is, if s_a and s_m are frame positions in the sequence for an automatic and manual sampling respectively, we define their distance as:

$$d = |s_a - s_m|$$

The distances of all frames provide a distance map for each patient. We consider the average of these distances to obtain a patient mean error. Statistical ranges ($\mu \pm \sigma$) of errors for all patients indicate the accuracy of our method.

B. Results

Table III-B reports error ranges for the two different band-pass filters, Butterworth and Gabor. Ranges are given in frames (first row), seconds (second row) and millimeters (third row).

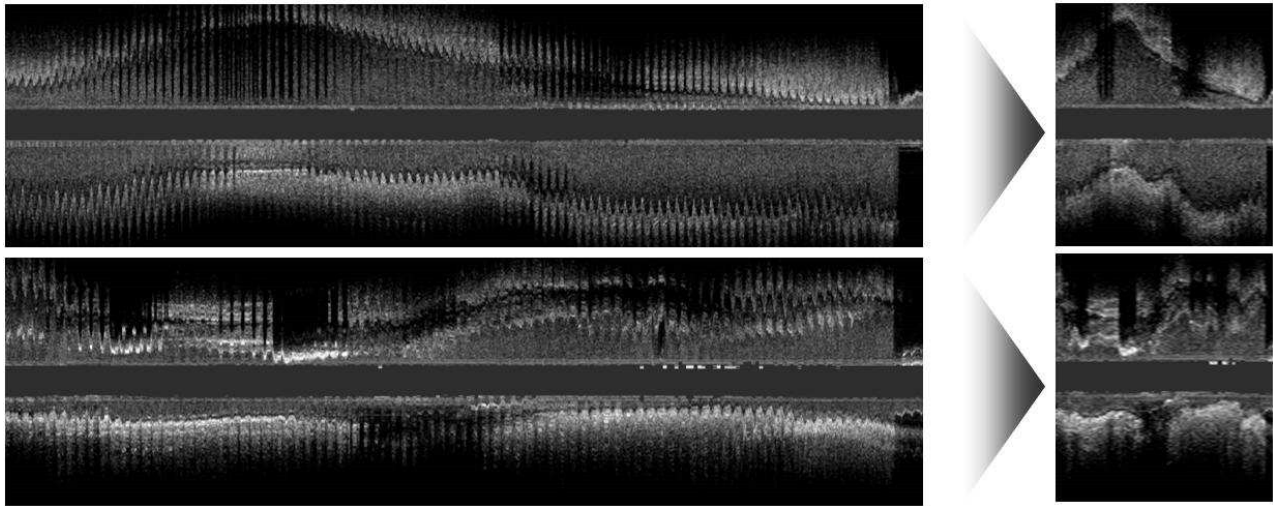


Figure 6. Image-based ECG sampling for two different longitudinal cuts.

Table I
RANGES FOR THE TWO DIFFERENT BAND-PASS FILTER

	Butterworth	Gabor
frames	14 ± 23	4 ± 4
seconds	0.47 ± 0.76	0.13 ± 0.13
millimeters	0.24 ± 0.38	0.07 ± 0.07

With the parameters given in section II, the filtered signals with Butterworth filter have an accuracy of at most 37 frames, which correspond to 0.62 mm. Meanwhile, the Gabor filter reports a better accuracy than Butterworth filter, with a maximum of 4 frames (0.14 mm.).

Figure 6 shows the performance of our method for the Gabor filtering in 2 large longitudinal cuts (left) sampled at end diastole rate (right). For the first segment, we can notice the continuous profile for the lumen contour, while in the second segment, we can follow up the calcium plaque present in the vessel.

IV. DISCUSSION AND CONCLUSIONS

In this paper, a methodology for retrieving cardiac phase has been presented. Exploring *LM* evolution is a fast way to extract cardiac signal from IVUS sequences. Strayed results for two different filters with given parameters show that filters play a relevant role for the method. Results for Gaussian-based signals encourage comparison to samplings obtained from ECG signals.

The parameters have been selected in reference to related work. However, since cardiac phase can be strongly affected by artery lesions and other cardiac factors, a study in depth of the filter parameters would check the robustness of the filters to a variety of subjects. This fact implies that a larger experimental setting would contribute to solid results.

ACKNOWLEDGEMENTS

This work was supported by the Spanish projects PI071188 and CONSOLIDER-INGENIO 2010 (CSD2007-00018). The last author has been supported by The Ramon y Cajal Program.

REFERENCES

- [1] A. Arbab-Zadeh, A. DeMaria, W. Penny, R. Russo, B. Kimura, and V. Bhargava, "Axial movement of the intravascular ultrasound probe during the cardiac cycle: implications for three-dimensional reconstruction and measurements of coronary dimensions," *Am. Heart J.*, vol. 138, pp. 865–872, 1999.
- [2] N. Bruining, C. von Birgelen, P. J. de Feyter, J. Ligthart, W. Li, P. Serruys, and J. R. Roelandt, "ECG-gated versus nongated three-dimensional intracoronary ultrasound analysis: implications for volumetric measurements," *Catheterization and Cardiovascular Diagnosis*, vol. 43, pp. 254–260, 1998.
- [3] C. von Birgelen, G. Mintz, A. Nicosia, D. P. Foley, W. J. van der Giessen, N. Bruining, S. Airiian, J. T. C. Roelandt, P. de Feyter, and P. Serruys, "Electrocardiogram-gated intravascular ultrasound image acquisition after coronary stent deployment facilitates on-line three-dimensional reconstruction and automated lumen quantification," *JACC*, vol. 30, no. 2, pp. 436–443, Aug. 1997.
- [4] S. A. de Winter, R. Hamers, M. Degertekin, K. Tanabe, P. Lemos, P. Serruys, J. R. Roelandt, and N. Bruining, "Retrospective image-based gating of intracoronary ultrasound images for improved quantitative analysis: The intelligate method," *Catheterization and Cardiovascular Interv.*, vol. 61, pp. 84–94, 2004.
- [5] S. . Nadkarni, D. . Boughner, and A. . Fenster, "Image-based cardiac gating for three-dimensional intravascular ultrasound imaging," *Ultrasound in Medicine and Biology*, vol. 31, no. 1, pp. 53–63, 2005.
- [6] H. Zhu, K. D. Oakeson, and M. H. Friedman, "Retrieval of cardiac phase from IVUS sequences," in *Medical Imaging 2003: Ultrasonic Imaging and Signal Processing*, vol. 5035, 2003, pp. 135–146.
- [7] M. M. S. Matsumoto, P. A. Lemos, T. Yoneyama, and S. S. Furuie, "Cardiac phase detection in intravascular ultrasound images," in *Proceedings*, October 2007.
- [8] J. Shaw, B. Kingwell, A. Walton, J. Cameron, P. Pillay, C. Gatzka, and A. Dart, "Determinants of coronary artery compliance in subjects with and without angiographic coronary artery disease," *JACC*, vol. 39(10), pp. 1637–1643, 2002.
- [9] S. Nadkarni, H. Austin, and et al., "A pulsating coronary vessel phantom for two and three-dimensional intravascular ultrasound studies," *Ultrasound Med. Biol.*, vol. 29 (4), pp. 621–628, 2003.
- [10] A. Hernández and D. Gil, "How do conservation laws define a motion suppression score in in-vivo ivus sequences?" in *2007 IEEE International Ultrasonics Symposium*, October 2007.
- [11] D. Gil, O. Rodriguez-Leor, P. Radeva, and J. Mauri, "Myocardial perfusion characterization from contrast angiography spectral distribution," *IEEE Trans. on Med. Imag.*, vol. 27, no. 5, pp. 641–649, 2008.
- [12] A. Klug and D. J. DeRosier, "Optical filtering of electron micrographs: reconstruction of one-sided images," *Nature*, vol. 212, pp. 29–32, 1966.